Impedance analysis of fibroblastic cell layers measured by electric cell-substrate impedance sensing

Chun-Min Lo* and Jack Ferrier
Medical Research Council Group in Periodontal Physiology, University of Toronto, Toronto, Ontario, Canada M5S 1A8
(Received 18 December 1997)

Impedance measurements of cell layers cultured on gold electrode surfaces obtained by electric cell-substrate impedance sensing provide morphological information such as junctional resistance and cell-substrate separation. Previously, a model that assumes that cells have a disklike shape and that electric currents flow radially underneath the ventral cell surface and then through the paracellular space has been used to theoretically calculate the impedance of the cell-covered electrode. In this paper we propose an extended model of impedance analysis for cell layers where cellular shape is rectangular. This is especially appropriate for normal fibroblasts in culture. To verify the model, we analyze impedance data obtained from four different kinds of fibroblasts that display a long rectangular shape. In addition, we measure the average cell-substrate separation of human gingival fibroblasts at different temperatures. At temperatures of 37, 22, and 4 °C, the average separation between ventral cell surface and substratum are 46, 55, and 89 nm, respectively.
[S1063-651X(98)04006-9]

PACS number(s): 87.22.−q, 87.80.+s

INTRODUCTION

The interactions between neighboring cells and between cells and their attached substrate have long been studied in tissue culture [1]. These *in vitro* studies may provide information regarding cell behavior *in vivo* including cell movement, cell proliferation, tissue development, and wound healing. In general, normal fibroblasts with an appropriate environment will proliferate and form a monolayer. As a consequence of contact inhibition of motion, these cells have a tendency to align with each other. Transcellular resistance (or impedance) measurements, using various dc or ac techniques, have been used to study the barrier function of epithelial and endothelial cell layers. With an appropriate equivalent circuit used for data analysis, junctional resistance between cells and other cellular properties, including cell membrane capacitance, can be determined. However, these techniques have seldom been applied to fibroblastic cell layers because the transcellular resistance is so small that it is difficult to measure it accurately.

Electric cell-substrate impedance sensing (ECIS) has been used to study cell motion and morphology in recent years [2–8]. In this method, cell layers are cultured on small gold electrodes and the electrical impedance of the cell-covered electrode is measured as a function of frequency. Comparing the experimental data with the calculated values obtained from a proper cell-electrode model, both junctional resistance and average cell-substrate separation can be acquired. Since the measured electrical resistance is very dependent on the extracellular space available for current flow, this method can detect morphological changes as small as a few nanometers. Previously, there have been two cell-electrode models used for impedance analysis of the frequency scan data measured by ECIS. One is appropriate for cells with lower junctional resistance, and has been applied to transformed fibroblastlike cells [2,3], and the other was used for cells with higher junctional resistance such as epithelial cells [7]. In these two models, cell shape is considered to be a disk, and the calculated values have been demonstrated to precisely fit the experimental data. However, the assumption of a disk shape is not appropriate for normal fibroblasts, which display a long and narrow shape. Application of a disk-shaped model to these cells would overestimate the average under-the-cell path length for current flow, and would lead to an overestimation of the cell-substrate distance when applied to measured data. A new model applicable to the shape of the normal fibroblast is therefore required.

In this study, we derive a model in which cell shape is assumed to be a rectangle with a half disk on each end. With the adjustment of both rectangular length and width, we use this model to analyze impedance data obtained from four different fibroblastic cell lines. We compare the results of this analysis to that obtained using the disk-shaped model. We also use this new model to analyze ECIS measurements done at different temperatures. We show that, as temperature decreases, the average cell-substrate separation of human gingival fibroblasts increases, and that this temperature effect is reversible. These results indicate that cell-substrate separation is dependent on metabolically controlled mechanisms of cell-substrate adhesion.

MATERIALS AND METHODS

Tissue culture

The fibroblast cell line WI-38 was obtained from the American Type Culture Collection (ATCC, Rockville, MD). Human gingival fibroblasts (HGF), human dermal fibro-

*Author to whom correspondence should be addressed. Address correspondence to MRC Group in Periodontal Physiology, 4384 Medical Sciences Building, University of Toronto, Toronto, Ontario, Canada M5S 1A8. FAX: (416) 978-5956. Electronic address: chunmin.lo@utoronto.ca

blasts, and normal foreskin fibroblasts were derived from primary explant cultures. Cells were cultured at 37 °C and 5% CO_2 in Dulbecco's modified Eagle medium (DMEM, GIBCO) with 10% fetal bovine serum (FBS, GIBCO) and antibiotics. Only cells from passages 3 to 6 were used for the experiments except WI-38 cells.

Impedance measurements

Electrode arrays, relay bank, lock-in amplifier, and software for the ECIS measurement were obtained from Applied BioPhysics (Troy, NY). Each electrode array consists of five wells that are 1 cm in height and 0.5 cm^2 in area; each well contains a 250-μm-diam gold electrode and a much larger gold counter electrode. For impedance measurements, medium (0.4 ml) was added over the electrode in each well. Experimental setup and circuit connection were the same as we previously described [7]. Cells were allowed to attach and spread for at least 24 h before impedance measurements were undertaken. We used an incubator without CO_2 and a normal refrigerator as 37 and 4 °C environments, respectively, and the room temperature was about 22 °C. Before taking data we waited at least 30 min after changing the temperature.

MODEL DERIVATION

List of Symbols

Z_c (Ω cm^2)	specific impedance (per unit area) of the cell-covered electrode
Z_n (Ω cm^2)	specific impedance of the cell-free electrode
Z_m (Ω cm^2)	specific impedance through both basal and apical cell membranes
V_c (V)	applied voltage across the cell-electrode system
I_{ct} (A)	total current through the area of a single cell
I_{ct}^{rec} (A)	total current through the rectangular part of a single cell
I_{ct}^{disk} (A)	total current through the disk part of a single cell
R_b^* (Ω)	junctional resistance between adjacent cells
R_b (Ω cm^2)	junctional resistance between adjacent cells over a unit cell area
ρ (Ω cm)	resistivity of the cell culture medium
L (μm)	cell length
W (μm)	cell width
h (nm)	average height between basal cell surface and substratum

The main objective of an ECIS model is to calculate the specific impedance of a cell-covered electrode as a function of frequency (Z_c) from the measured values of a cell-free electrode (Z_n) with a few suitable morphological parameters of cell layers. After fitting the measured data of the same electrode covered with cells with the calculated values of Z_c, those morphological parameters can be determined. Therefore, the total current passing through the area of a single cell (I_{ct}) as a function of the applied electrode voltage (V_c) must be first calculated, and then Z_c can be obtained by the simple formula, $Z_c = (\text{cell area})(V_c/I_{ct})$.

In order to theoretically calculate Z_c, we simply assume that the cell shape is just like a rectangle with a half-disk on each end. As shown in Fig. 1(a), by geometrically separating the cell area into a rectangle and a disk, then individually calculating the current from each part, I_{ct}^{rec} and I_{ct}^{disk}, the total current passing through the area of a single cell, I_{ct}, therefore, can be obtained from the summation of the two values (i.e., $I_{ct}=I_{ct}^{\mathrm{rec}}+I_{ct}^{\mathrm{disk}}$). To calculate the total current flowing through the rectangular part of a single cell, I_{ct}^{rec}, we also assume that, in the spaces between cell and the substratum, current coming from the electrode will either go through the cell membranes (transcellular current) or one-dimensionally and symmetrically flow to the edges of the cell, and then through the paracellular space between cells (paracellular current). From Fig. 1(b) and Ohm's law we obtain

$$-\frac{dV}{dx}=\frac{\rho}{hL}I, \tag{1}$$

$$V_c-V=\frac{Z_n}{L\,dx}\,dI_c, \tag{2}$$

$$V=\frac{Z_m}{L\,dx}\,dI_i, \tag{3}$$

and

$$dI=dI_c-dI_i. \tag{4}$$

Equations (1)–(4) can be combined to yield the following differential equation:

$$\frac{d^2V}{dx^2}-\gamma^2V+\beta=0, \tag{5}$$

where

$$\gamma^2=\frac{\rho}{h}\left(\frac{1}{Z_n}+\frac{1}{Z_m}\right) \tag{6}$$

and

$$\beta=\frac{\rho V_c}{hZ_n}. \tag{7}$$

The general solution of Eq. (5) is

$$V=Ae^{\gamma x}+Be^{-\gamma x}+\frac{\beta}{\gamma^2}. \tag{8}$$

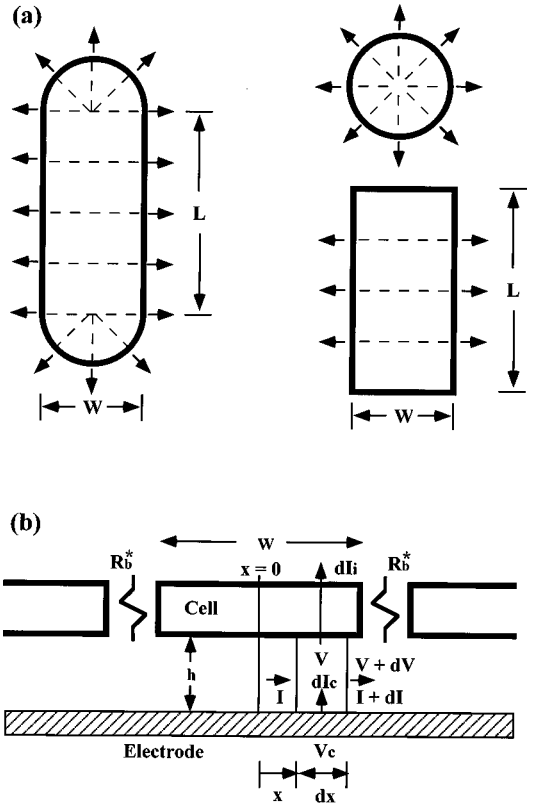

FIG. 1. A schematic diagram of the cell-electrode model for cell layers cultured on a gold electrode. Cells are considered as a flat rectangular ($L\times W$) box with a half disk ($r_c=W/2$) on each end, and the cell area is $LW+\pi W^2/4$. (a) Top view of the cell layer, where the total current flowing from the area of a single cell, I_{ct}, can be calculated as the summation of the current from both the disk and the rectangle parts of the cell; (b) side view of the cell layer emphasizing the cell-substrate spaces.

With two boundary conditions

$$I(x=0)=0 \tag{9}$$

and

$$I(x=W/2)\times 2R_b^{\text{rec}*}=V(x=W/2), \tag{10}$$

we can determine the two constants A and B. The final result of current flowing from the rectangular part of a single cell is calculated as

$$I_{ct}^{\text{rec}}=2\int_0^{W/2} dI_c$$

$$=\frac{LWV_c}{Z_n+Z_m}\times\left[1+\frac{\dfrac{2Z_m}{Z_n}}{\gamma W\coth\left(\dfrac{\gamma W}{2}\right)+2R_b^{\text{rec}}\left(\dfrac{1}{Z_n}+\dfrac{1}{Z_m}\right)}\right], \tag{11}$$

where

$$\frac{\gamma W}{2}=\frac{W}{2}\left[\frac{\rho}{h}\left(\frac{1}{Z_n}+\frac{1}{Z_m}\right)\right]^{1/2}=\alpha\left[\left(\frac{1}{Z_n}+\frac{1}{Z_m}\right)\right]^{1/2} \tag{12}$$

and

$$R_b^{\text{rec}}=WLR_b^{\text{rec}*}. \tag{13}$$

From the previous disk model [2,3], if the cell radius (r_c) is $W/2$, the total current flowing through a disk-shaped cell is

$$I_{ct}^{\text{disk}}=\frac{\dfrac{\pi W^2}{4}V_c}{Z_n+Z_m}\left[1+\frac{\dfrac{2Z_m}{Z_n}}{\dfrac{\gamma W}{2}\dfrac{I_0(\gamma W/2)}{I_1(\gamma W/2)}+2R_b^{\text{disk}}\left(\dfrac{1}{Z_n}+\dfrac{1}{Z_m}\right)}\right], \tag{14}$$

where I_0 and I_1 are modified Bessel functions of the first kind of order 0 and 1, and

$$R_b^{\text{disk}}=\frac{\pi W^2}{4}R_b^{\text{disk}*}. \tag{15}$$

From the equation, $Z_c=V_c(LW+\pi W^2/4)/I_{ct}$, the specific impedance of the cell-covered electrode can be resolved as

$$\frac{1}{Z_c}=\frac{1}{Z_n+Z_m}\left\{\begin{array}{l}1+\left(\dfrac{LW}{LW+\dfrac{\pi W^2}{4}}\right)\dfrac{\dfrac{2Z_m}{Z_n}}{\gamma W\coth\left(\dfrac{\gamma W}{2}\right)+2R_b^{\text{rec}}\left(\dfrac{1}{Z_n}+\dfrac{1}{Z_m}\right)}\\ +\left(\dfrac{\dfrac{\pi W^2}{4}}{LW+\dfrac{\pi W^2}{4}}\right)\dfrac{\dfrac{2Z_m}{Z_n}}{\dfrac{\gamma W}{2}\dfrac{I_0(\gamma W/2)}{I_1(\gamma W/2)}+2R_b^{\text{disk}}\left(\dfrac{1}{Z_n}+\dfrac{1}{Z_m}\right)}\end{array}\right., \tag{16}$$

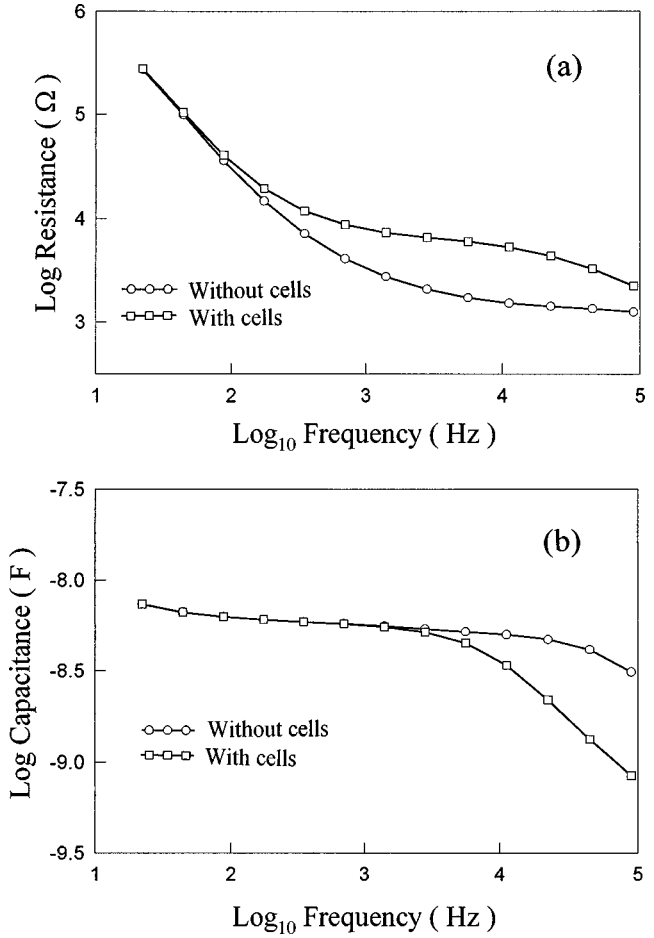

FIG. 2. (a) Resistance and (b) capacitance as a function of $\log_{10}$(frequency) obtained from a frequency scan measurement of an electrode with and without a monolayer of HGF cells.

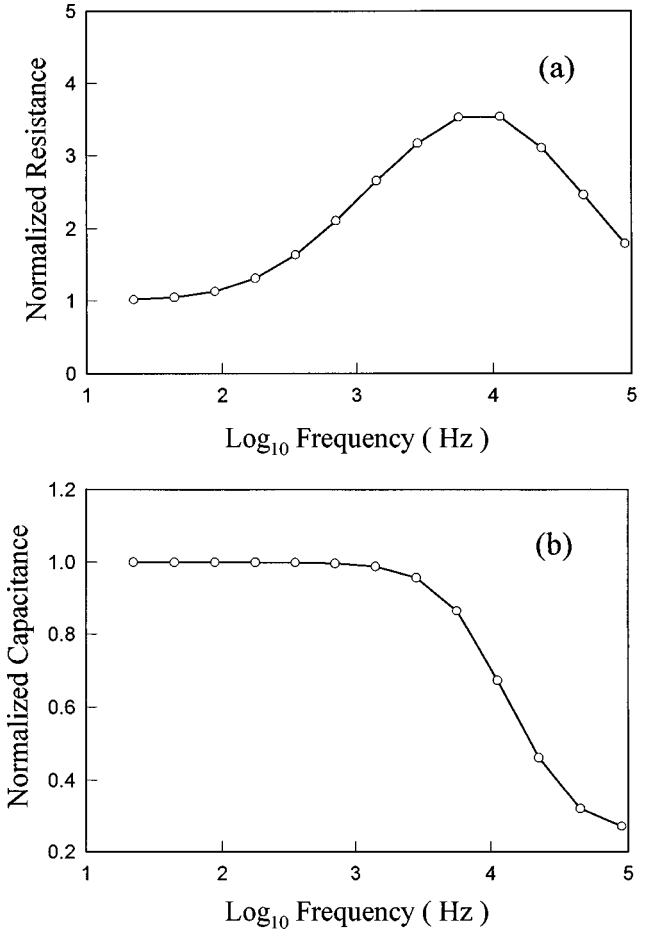

FIG. 3. (a) Normalized resistance and (b) normalized capacitance as a function of $\log_{10}$(frequency) for an electrode with a confluent HGF cell layer. The curves are obtained from Fig. 2 by dividing the measured values for the cell-covered electrode by the corresponding values for the cell-free electrode.

where

$$R_b^{\mathrm{rec}}=\frac{\frac{4L}{W}+2\pi}{\frac{4L}{W}+\pi}R_b \tag{17}$$

and

$$R_b^{\mathrm{disk}}=\frac{\frac{2L}{W}+\pi}{\frac{4L}{W}+\pi}R_b\,. \tag{18}$$

There are two limiting cases. First, if $L\gg W$, then $R_b^{\mathrm{rec}}\approx R_b$, $I_{ct}\approx I_{ct}^{\mathrm{rec}}$, and the rectangular part of cell dominates the measured impedance. Second, if $L\approx 0$, $R_b^{\mathrm{disk}}\approx R_b$, $I_{ct}\approx I_{ct}^{\mathrm{disk}}$ and the result returns to the previous calculation obtained from the disk model.

RESULTS AND DISCUSSION

Figure 2 shows measured resistance and capacitance as a function of frequency. These curves show results for both cell-free electrodes and for electrodes covered with a confluent layer of HGF cells, at 37 °C. For analyzing differences in impedance curves, it is helpful to use normalized values, where we divide the impedance values of cell-covered electrodes by the corresponding quantities of the cell-free electrodes. Figure 3 displays normalized resistance and capacitance data for HGF cells. The theoretical model can be fit to the measured normalized impedance with adjustment of two parameters, R_b and α. Cell length (L) and width (W) can be estimated directly by phase-contrast microscopy, and the specific impedance of the cell membrane (Z_m) can be calculated as a resistor (membrane resistance) and a capacitor (membrane capacitance) in parallel, as we described before [7,8]. Using Eq. (16) to analyze normalized resistance and capacitance curves of HGF cells, the best-fitting values of R_b and α for the data shown in Fig. 3 are 1.4 Ω cm^2 and 2.4 Ω$^{1/2}$ cm. We calculate h from α by using Eq. (12) with $\rho=54$ Ω cm and $W=14$ μm. The result for the average cell-substrate separation at 37 °C is 46 nm. Comparing this to the result obtained by fitting the model based on a disk-shaped cell to these data (Table I), the average cell-substrate value from the rectangular model is much closer to the results measured by interference reflection microscopy (IRM) [9,10].

Before analyzing more experimental data, it is helpful to know how changes of R_b and α affect the normalized curves.

TABLE I. Impedance analysis of HGF cells from two different models at 37 °C.

	ρ (Ω cm)	R_b (Ω cm^2)	α ($\Omega^{1/2}$ cm)	h (nm)
Disk model ($r_c=18\ \mu$m) [$\alpha=r_c(\rho/h)^{1/2}$]	54	1.5	3.7	128
Rectangular model ($W=14\ \mu$m) [$\alpha=0.5W(\rho/h)^{1/2}$]	54	1.4	2.4	46

Figure 4 shows the normalized resistance and capacitance as a function of frequency for a range of R_b values: 0.5, 1, 2, and 3 Ω cm^2, with $L=70\ \mu$m, $W=14\ \mu$m, $\alpha=2.4\ \Omega^{1/2}$ cm, and $C_m=2\ \mu$F/cm^2. When R_b increases, the normalized resistance values increase and the peaks of all the curves are almost at the same frequency position. Figure 5 shows another calculation where α takes on the values of 2, 3, 4, and 5 $\Omega^{1/2}$ cm, $R_b=1.5\ \Omega$ cm^2, and C_m has the same value as in Fig. 4. The normalized resistance values increase while α increases; however, the peak of the data curve shifts to the low-frequency side. Since the parameter α is inversely proportional to $h^{1/2}$, the peak position of the normalized resistance curve strongly depends on cell-substrate separation. Comparing the normalized capacitance curves in Fig. 4(b) with those in Fig. 5(b), we see that they also vary in different ways as the parameters R_b or α change. It is worthwhile to mention here that the capacitance measured by ECIS is the capacitance of the electrode-electrolyte interface. At high frequency the capacitance becomes smaller when cells cover up some of the electrode area. At low frequency, however, the capacitance does not change much even when there are cells on the electrode because there is sufficient time to change the capacitive charge under the cell. Therefore, when R_b increases or h decreases (i.e., α increases), capacitance values at higher frequencies decrease, as a result of less current coming out of the electrode, but those at low frequencies change only a little.

We carried out a series of measurements of the transcellular impedance of confluent fibroblast cell layers at 37, 22,

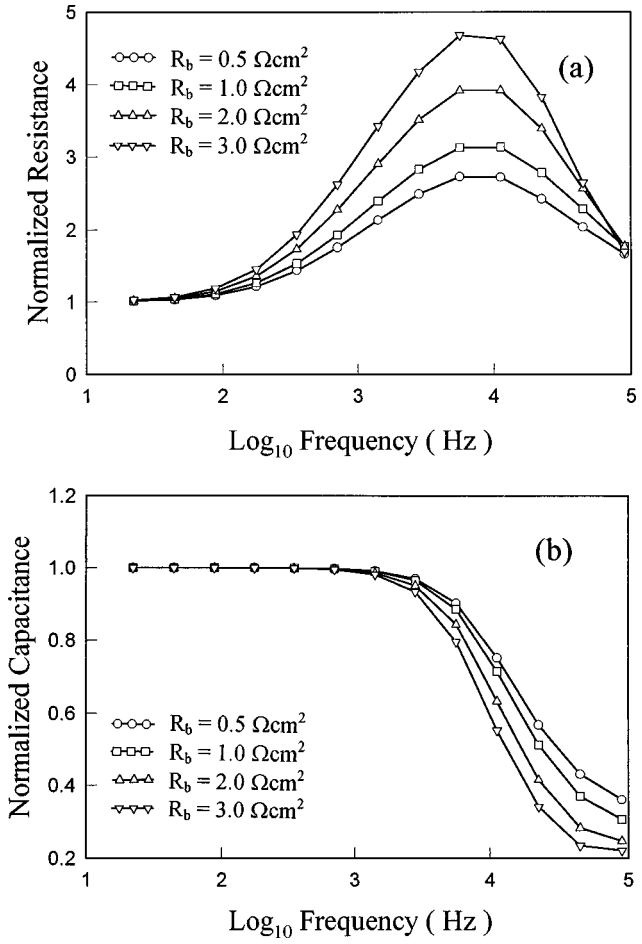

FIG. 4. (a) Normalized resistance and (b) normalized capacitance as a function of $\log_{10}$(frequency) from model calculations for different junctional resistances, R_b: 0.5, 1, 2, and 3 Ω cm^2. The parameters α and C_m were set to 2.4 $\Omega^{1/2}$ cm and 2 μF/cm^2, respectively; these values are close to the experimental results for HGF cells.

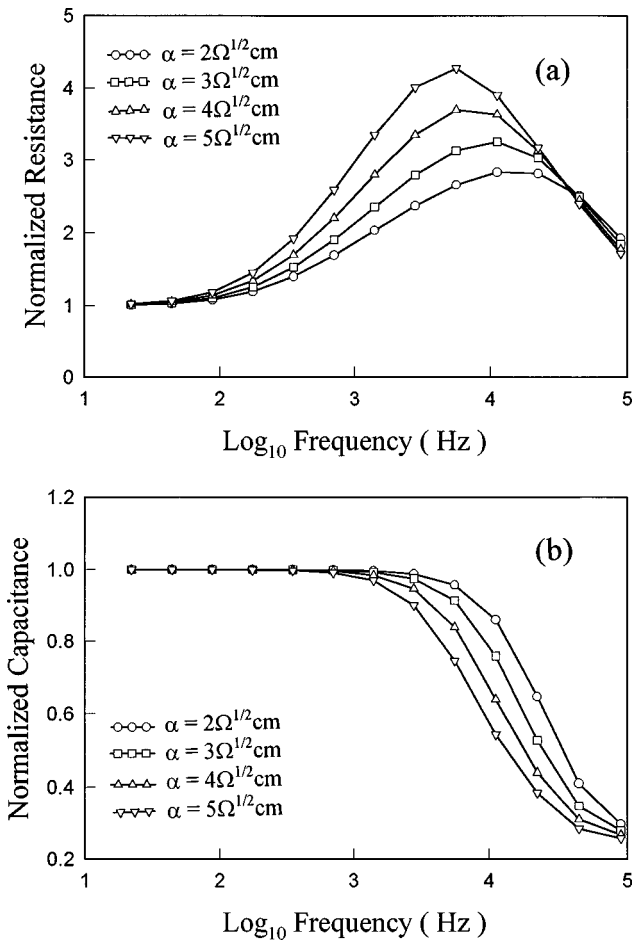

FIG. 5. (a) Normalized resistance and (b) normalized capacitance as a function of $\log_{10}$(frequency) from model calculations for different values of the parameter α: 2, 3, 4, and 5 $\Omega^{1/2}$ cm. The other parameters R_b and C_m were set to 1.5 Ω cm^2 and 2 μF/cm^2, respectively.

TABLE II. Effect of temperature on cell-substrate separation of HGF cells. Using the new fibroblast model, two parameters are used to fit the measured cell layer impedance as a function of frequency: R_b, which is the junctional resistance between cells, and $\alpha = 0.5W(\rho/h)^{1/2}$, where W is cell width, ρ is the extracellular medium resistivity, and h is the average cell-substrate separation. The number of independent measurements at each temperature is given by n. The $\pm$ values are estimates based on both the reproducibility of the impedance measurements and the sensitivity of the model impedance curves to the parameters.

	ρ (Ω cm)	R_b (Ω cm^2)	α ($\Omega^{1/2}$ cm)	h (nm)
37 °C ($n=10$)	54	1.4 ± 0.1	2.4 ± 0.1	46 (42–50)
22 °C ($n=10$)	70	1.7 ± 0.1	2.5 ± 0.1	55 (51–60)
4 °C ($n=10$)	114	2.9 ± 0.1	2.5 ± 0.1	89 (83–97)

and 4 °C and analyzed the data as described above. The impedance of cell-free electrodes was also measured at these temperatures. The best values of R_b and α to fit the experimental data are shown in Table II. To calculate the average cell-substrate separation, h, we use the same value of W, 14 μm, at all three temperatures. The reason for this is that our results show the junctional resistance between cells, R_b, to be proportional to the medium resistivity, ρ, which increases as the temperature decreases. This implies that there is little effect of temperature on the intercellular spacing, with the changes of R_b being attributable to the changes of the medium resistivity. Estimates for the uncertainty in our measured values for h are also shown in Table II. These estimates are based on both the precision of the data and the sensitivity of the procedure for fitting the model to the data. The average distance between the ventral cell surface and substrate, h, increases from 46 to 55 to 89 nm as the temperature decreases from 37 to 22 to 4 °C (Table I). This result suggests that the area of close contact between cell and substrate decreases as temperature decreases, since the ECIS measurement for h gives the average separation of the ventral surface from the substrate, including the close contact areas as well as the areas that are not as close. This agrees with the results of Lotz *et al.* [11], who showed in an IRM study of glioma cell adhesion to fibronectin that the focal contact area (with cell-substrate separation $\leqslant 15$ nm) is less at 4 than at 37 °C. It should be noted that this temperature effect on cell-substratum interaction can be reversibly repeated. From our previous results [8], this temperature effect can be explained on the basis that the number of adhesion bonds per cell decreases while temperature decreases.

TABLE III. Using the new model with three other fibroblast types. All values, $\alpha[=0.5W(\rho/h)^{1/2}]$ and R_b, obtained from impedance measurements at 37 °C.

	R_b (Ω cm^2)	α ($\Omega^{1/2}$ cm)	h (nm)
WI-38 fibroblasts ($L=60$ μm, $W=12$ μm)	0.5	2.4	34
Normal foreskin fibroblast ($L=100$ μm, $W=16$ μm)	0.6	2.2	71
Human dermal fibroblasts ($L=120$ μm, $W=18$ μm)	2.2	3.6	34

We also analyzed impedance data obtained from other fibroblastic cell types and the results are shown in Table III. Our results show that the junctional resistance of these fibroblasts is in the range of $0.5-2.5$ Ω cm^2, and their average cell-substrate distances are from 30 to 80 nm, very close to those values obtained from IRM measurements. In general, comparing to other cell types such as epithelial and endothelial cell layers, the junctional resistance of fibroblastic cell layers is very small, in a range that other methods are not sensitive enough to detect.

The model developed here can be used in future studies of the adhesion properties and the degree of cell-to-cell contact of fibroblasts. Such cell-to-substrate (or cell-to-extracellular matrix) and cell-to-cell interactions are of prime importance in regulating the function of these cells.

[1] F. Grinnell, Int. Rev. Cytol. **53**, 65 (1978).
[2] I. Giaever and C. R. Keese, Proc. Natl. Acad. Sci. USA **88**, 7896 (1991).
[3] I. Giaever and C. R. Keese, Proc. Natl. Acad. Sci. USA **90**, 1634 (1993).
[4] I. Giaever and C. R. Keese, Nature (London) **366**, 591 (1993).
[5] C.-M. Lo, C. R. Keese, and I. Giaever, Exp. Cell Res. **204**, 102 (1993).
[6] C.-M. Lo, C. R. Keese, and I. Giaever, Exp. Cell Res. **213**, 391 (1994).
[7] C.-M. Lo, C. R. Keese, and I. Giaever, Biophys. J. **69**, 2800 (1995).
[8] C.-M. Lo, M. Glogauer, M. Rossi, and J. Ferrier, Eur. Biophys. J. **27**, 9 (1998).
[9] M. Abercrombie, J. E. M. Heaysman, and S. M. Pegrum, Exp. Cell Res. **67**, 359 (1971).
[10] C. S. Izzard and L. R. Lochner, J. Cell. Sci. **21**, 129 (1976).
[11] M. M. Lotz, C. A. Burdsal, H. P. Erickson, and D. R. McClay, J. Cell Biol. **109**, 1795 (1989).